ISSN: 0067-2904

Application of SEM and Petrographic Studies to Reservoir Characterisation of the Eze-Aku Sandstone (Afikpo Sub-basin), South-eastern Nigeria

Omabehere Innocent Ejeh[1*], Minapuye Isaac Odigi [2]
[1]*Department of Geology, Delta State University, Abraka, Nigeria*
[2]*Department of Geology, University of Port Harcourt, Port Harcourt, Nigeria.*

Received: 3/12/2020 Accepted: 31/8/2021 Published: 30/9/2022

Abstract

The reservoir characteristics of the Pre-Santonian Eze-Aku sandstone were assessed using an integrated thin section petrography and SEM Back-Scattered Electron (BSE) imaging methods. Fresh outcrop data were collected in the Afikpo area (SE Nigeria). Twenty-eight representative samples from the different localities were analysed to obtain mineralogical and petrographical datasets germane for reservoir characterisation. Thin section petrography indicates that the sandstones are medium-grained, have an average $Q_{90}F_{10}L_0$ modal composition, and are classified as mainly sub-arkose. The sandstones on SEM reveal the presence of cement in the form of quartz overgrowths, authigenic clays and feldspar. From epoxy-stained thin sections and/or SEM BSE image analysis, primary, secondary (inferred from partial to total feldspar dissolution/alteration), and micro- (in authigenic clays) porosity types were identified. Although the development of quartz overgrowths, authigenic clay precipitation, and feldspar dissolution often affect reservoir properties of sandstone negatively, the Eze-Aku sandstones still retained very good reservoir properties (porosity, average 22.7 %; permeability, average 745.43 mD). This can be attributed to the abundance of framework grains that have been stabilized by quartz cement and relatively limited feldspar dissolution. The stabilized framework grains help preserve reservoir characteristics and resist further compaction beyond eogenetic depths. The feldspar dissolution produced silica and aluminium that was precipitated to form the quartz overgrowths and the authigenic clays (e.g., kaolinite), respectively. The relatively concurrent precipitation of silica and aluminium from dissolution products reduces the quartz overgrowth quantity and authigenic clays that could have adversely affected the reservoir characteristics.

Keywords: SEM BSE images, diagenesis, porosity, authigenic clay minerals, Eze-Aku sandstone

Introduction

The existence of an active reservoir rock or an unconventional reservoir rock is an invaluable element of the petroleum system concerning hydrocarbon exploration, development, and production [1] [2] [3]. The reservoir quality depends on the sedimentary depositional processes (such as diagenesis) and environment (s). Textural and mineralogical characteristics of clastic sedimentary rocks such as sandstones are strong indices of reservoir quality prediction [4] [5]. However, during burial, diagenetic processes affect the petrophysical characteristics; the fabric and the sand mineralogy being lithified to sandstones are often altered [5]. The tectonic setting, depositional facies, burial depths, mineralogical

*Email: ejehoi@gmail.com

composition, basin fluids composition and flow pattern all control the diagenetic pattern and reservoir-quality evolution pathways [5].

The sedimentology and the reservoir quality of two out of the three main sequences of the Afikpo basin (located in south-eastern Nigeria); the Asu River and Nkporo Groups, have been studied [6] [7] [8]. The third Group, the Eze-Aku, was reported as a shallow marine environment [9], most likely made up of tidal deposits [10]. However, Amajor [11], based on facies analysis of the sandstones of the Eze-Aku, held a contrary view that they are not tide-dominated but rather storm-dominated.

In the third sequence, the Eze-Aku Group faced a dearth of research information on diagenesis and reservoir quality of the pre-Santonian Eze-Aku sandstones of the Afikpo sub-basin. The objectives of this paper are to elucidate the reservoir characteristics of the marine and non-marine sandstones of the Eze-Aku Sandstones and discuss diagenetic processes that affected the sandstones' reservoir quality in the Afikpo Basin. These objectives are key deliverables in the exploration and development activities of oil and gas in Nigeria's inland Cretaceous sedimentary basin.

Geological Setting

The tripartite (southern, middle, and northern) aulacogen Benue Trough (Figure 1) was affected by the Santonian tectonic activity that caused basin inversion and subsequently formed the Anambra Basin and the Afikpo sub-basin to the north-west and south-east respectively [12] [13]. The Afikpo basin is located east of the southern Benue Trough (Figure 1), which has the Abakaliki Anticlinorium. The Santonian deformation episode constitutes a basis for classifying the sedimentary successions of the basin into pre-and post-

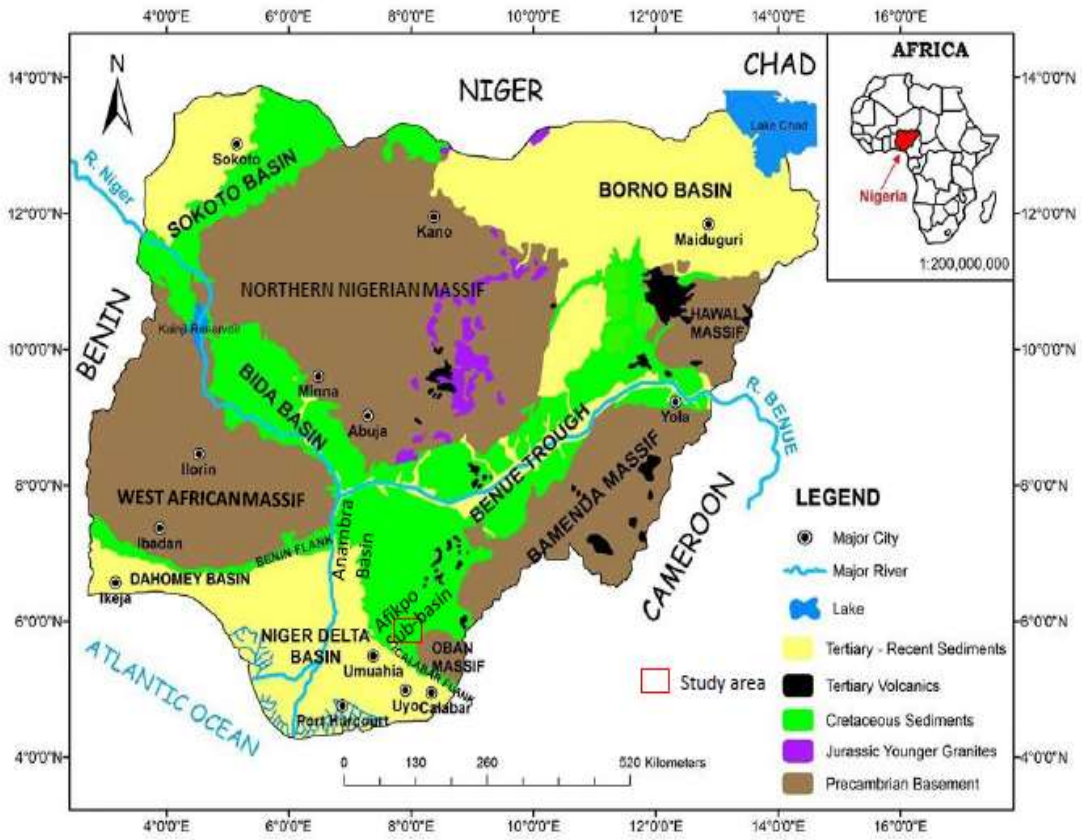

Figure 1- Geological map of Nigeria, modified after [14]; study area marked in a rectangle to the south-east.

Santonian sedimentary packages. The Asu River and Eze-Aku Groups belong to the pre-Santonian sequences in the southern Benue Trough. The pre-Santonian Eze-Aku Sandstones are strongly deformed, unlike the post-Santonian successions that are moderately dipping. In the Afikpo sub-basin, both Cenomanian and Santonian tectonism affected the pre-Santonian successions [15] [16] [17] [18]. Figures 2 and 3 show the Cretaceous stratigraphic successions and geologic map of the study area, respectively.

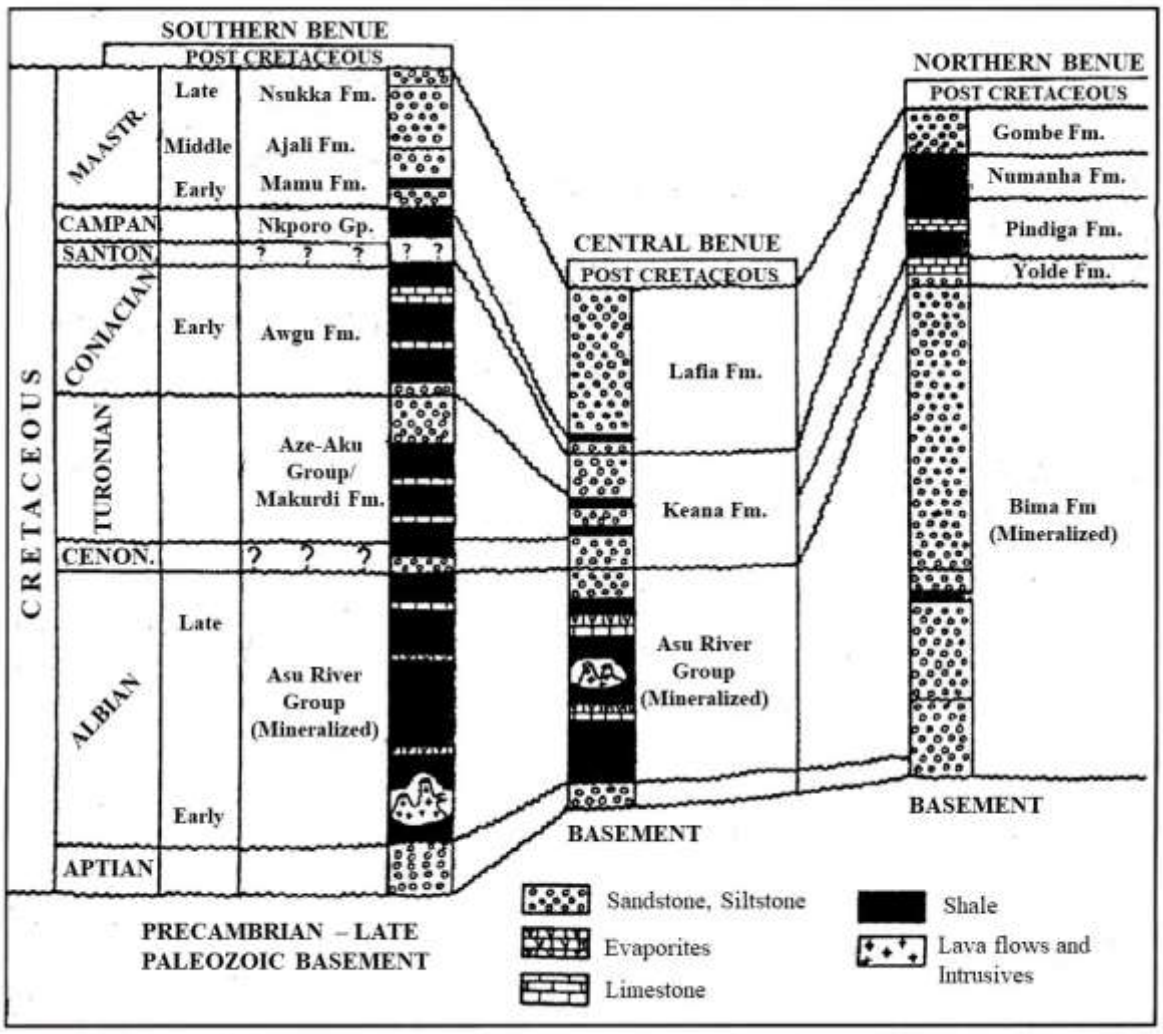

Figure 2- Composite Cretaceous stratigraphy of the Benue Trough, including Afikpo Sub-basin (Simplified by [19]).

The depositional framework of the Eze-Aku Group

The Afikpo sub-basin fill consists of three mega sequences; the Albian-Cenomanian, Asu-River Group; the Turonian-Coniacian, Eze-Aku Group; and the Campanian-Maastrichtian Nkporo Group. The Eze-Aku Group consists of Amasiri Sandstone and several other stratigraphic sandstone bodies (e.g., Ibii, Amaoru, Abaomega, Imina, Ugep, Ozara Ukwu, Idomi, Abini, Ofat, Nko, and Akpoha Igbo and Agbara Igbo), limestones, and shales. These sandstone bodies occur as ridges (e.g., Amasiri-Abaomega ridge) with dark shales and limestones that are parallel and elongate, striking NE-SW and E-W with dips ranging from 35° to 68° (Figure 4). The lithostratigraphic units of the Eze-Aku Group alongside their known depositional environment, are summarised in Table1.

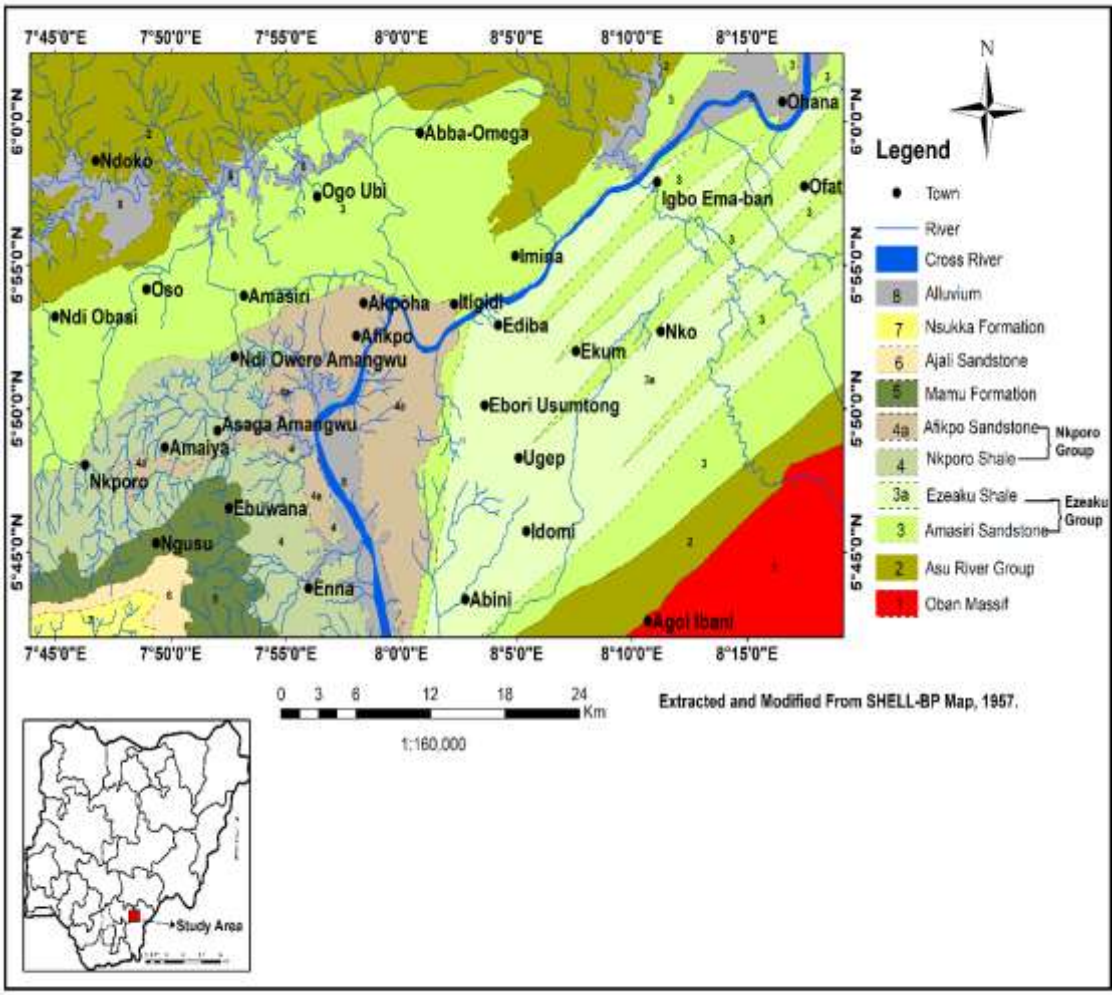

Figure 3- Geological map of the study area, after [8]; insert is a map of Nigeria.

The Eze-Aku Sandstones have internal characteristics similar to shoreface deposits and are therefore interpreted as barrier island shoreface-foreshore sand-ridges [15]. In the study area, particularly under the old abandoned bridge across the Abaomega River in Akpoha, the dominantly exposed Eze-Aku shale has an average high dip value of 60°, and the facies changed to a sequence of sandstones interbedded with shales containing ammonites suggestive of shallow marine shelf depositional setting [20]. The Eze-Aku is dominantly a succession of sandstones, calcareous sandstones, shales, and siltstone facies (Table 1). The NE-SW trending ridges (Figure 4 a) of the sandstone facies occur in association with the low-lying plain of shales (swales) [20]. The notable sedimentary structures ubiquitous in the sandstones of the Eze-Aku include basal lag deposits (with a fining upward succession) (Figure 4 b) and planar cross-bedding (Figure 4 c-d)

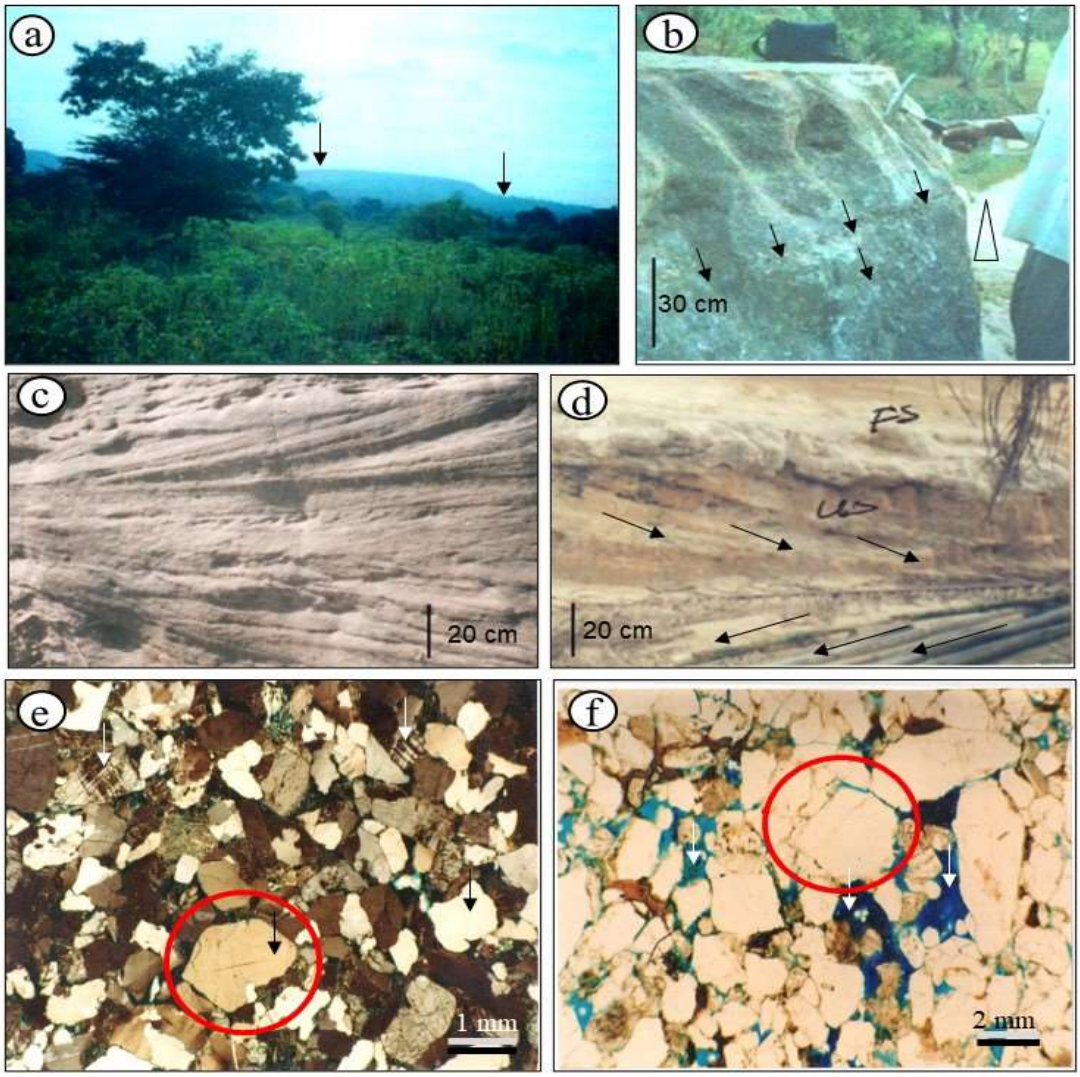

Figure 4- Field photographs and photomicrographs from the Eze-Aku sandstone [a-b and c-d exposed at Ozara and Agbara Igbo respectively] (a) Overview of the Ozara sandstone ridge (black arrows), (b) Fining upward sequences (1.5m thick) with lag basal deposits (indicated with black arrows), (c) Coarse grained sandstone with tabular cross beds, (d) Medium-fine grained sandstones with planar cross-beds (bidirectional, indicated with arrows). (e) Sub-arkose with microcline (white arrow), quartz (black arrow), other minerals, and grain to grain contacts (red circle) >5 [cross polarized light], and (f) Sub-arkose (exposed at Abini) with moderate intergranular porosity (white arrow) shown through impregnation with blue resin epoxy; grain to grain contacts (red circle) >5 [cross polarized light].

Table 1- Lithostratigraphy of the Eze-Aku Group.

Group	Stratigraphic units	Age	Lithologies	Depositional Environment
Eze-Aku Group	Agbara-Igbo Sandstone	Late Cenomanian - Turonian	Calcareous bioturbated Well sorted sandstone.	R-T barrier sand bodies.
	Abini Sandstoe		Calcareous bioturbated sandstone.	Shoreface.
	Ugep sandstone Formation		Bioturbated well sorted sandstone.	Shoreface.
	Ibii Sandstone		Bioturbated fine to medium sandstone	R-T barrier sand bodies.
	Abaomega Sandstone		Bioturbated fine to medium sandstone	R-T barrier sand bodies.
	Nko Sandstone		Bioturbated Sandstone.	Shoreface.
	Amasiri Sandstone		Calcareous Bioturbated sandstone.	Shoreface.
	Ezillo Sandstone		Bioturbated Sandstone	Shoreface.
	Eze-Aku Shale		Shale with ammonites.	Shallow marine.
R-T: Regressive-Transgressive barrier sand bodies				

Materials and Methods

A geological field mapping of the Afikpo area was done (Figure 3). Fresh sandstone outcrop samples (n=28) (Figure 5) were obtained and subjected to thin-section petrographic and scanning electron microscopic (SEM) analyses. Thin section analytical procedures involved slide cutting and staining [21] (with Alizarin red-s, K-ferricyanide, and Na-cobaltinitrite; for enhanced identification of feldspars) and point counting (300 points/slide) for modal analysis. Epoxy blue was injected into the thin sections to highlight pore spaces. Eight selected sandstone samples were examined using SEM on a back-scattered electron (BSE) mode to gain insight into the associated minerals and porosity values. The SEM analysis was performed at the Department of Earth Sciences, University of Liverpool, UK, using a JEOL-JSM6460LV SEM attached to the INCA Micro-analyser system. The samples were analysed using the Back-scatter Electron Image (BSEI), with some use of secondary electron image (SEI). The details of the principles and procedures/applications of SEM and BSE imaging are reported in [22] [23] [24]. The SEM BSE images were analysed using the open-source software package, ImageJ, developed by Rasband, W.S. of the U.S. National Institute of Health in 1997 [25].

Porosity and other relevant petrophysical parameters were estimated on ImageJ, and permeability was calculated from the estimated data using the Kozeny-Carman (K-C) equation.

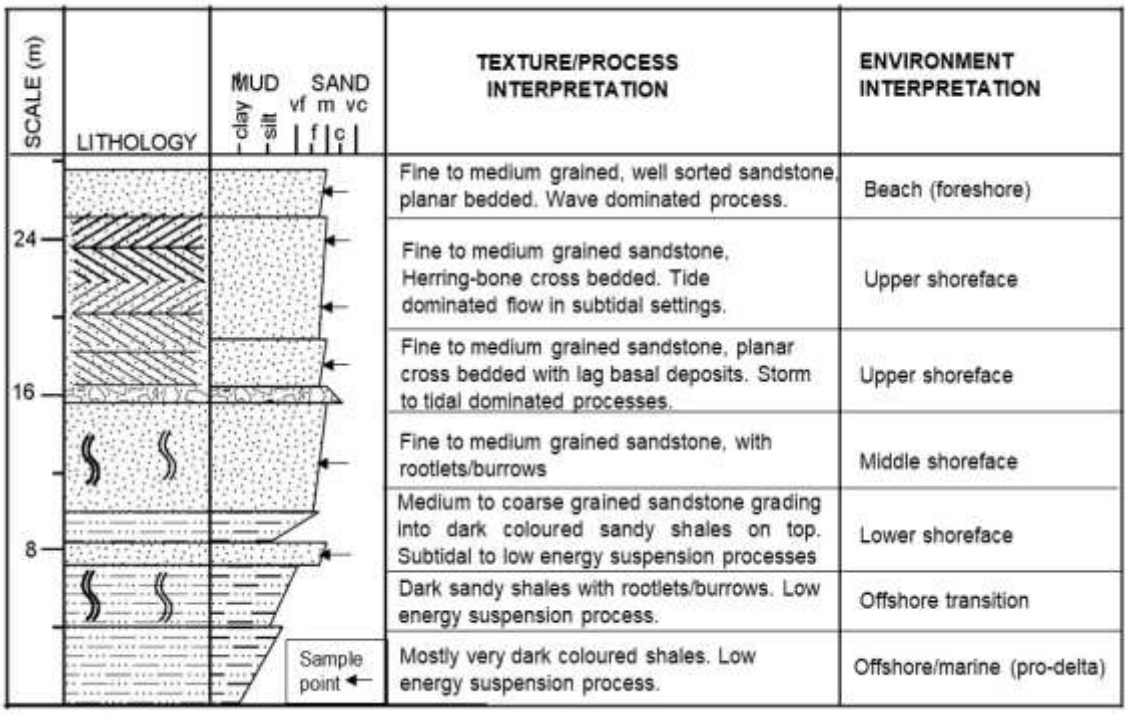

Figure 5- Composite lithological section from the Agbara-Igbo and Abaomega areas of the Turonian Eze-Aku sandstone.

Results

Mineralogical composition of the Eze-Aku Sandstones

Framework grains

In terms of grain size, the Eze-Aku sandstones are fine to medium-grained, moderately sorted, and occasionally display grain size-induced laminations. The 28 sandstone samples from the Eze-Aku have an average modal composition of $Q_{90}F_{10}L_0$ (Table 2), indicative of mostly sub-arkose sandstones on a QFL plot (Figure 6) [26]. However, there are some variations in the compositions in the different localities. For example, at Ibii and Ugep, modal compositions of the samples are quartz arenitic, while in the other localities, they are mostly sub-arkose sandstones (Table 2). The sub-arkose comprised quartz (mono- and polycrystalline), feldspar (microcline, orthoclase) and other accessory minerals (Figure 4 e&f). The moderate intergranular porosity (white arrow) shown through impregnation with blue resin epoxy; is evident from the partially altered plagioclase felspar grains visible in thin sections (Figure 4 f).

Table 2- Modal composition of the Eze-Aku sandstones.

Lithology/Facies	Locality	Quartz (mc)	Quartz (pc)	Feldspar (Kf)	Feldspar (Pf)	Lithic fragments
R-T bioturbated sandstone	Ibii	90	4	3	3	0
R-T bioturbated sandstone	Abaomega	90	0	5	5	0
Deltaic bioturbated sandstone.	Ugep	94	0	6	0	0
R-T calcareous bioturbated fine-medium sandstone	Amasiri	88	0	12	0	0
Deltaic bioturbated sandstone	Abini	83	5	7	5	0
Deltaic bioturbated sandstone	Nko	86	3	3	8	0
Tidal channel sandstone	Akpoha Igbo & Agbara Igbo	09	79	10	2	0
Cross-bedded channel sandstone	Ozara Ukwu	82	5	8	5	0

Channel sandstone =3, Tidal channel =3, Deltaic sandstone =10, calcareous bioturbated sandstone =4, and shoreface (R-T) = 8 samples; mc = monocrystalline quartz; pc = polycrystalline quartz, Kf = K-feldspar; Pf= Plagioclase feldspar.

The monocrystalline, well-rounded, and non-undulose quartz grains dominate the framework grains. The monocrystalline range from 09 to 94 % (average 77.7%), and polycrystalline quartz ranges from 0 to 79% (average 12.0 %). The K-feldspar ranged from 3 to 12 % (average 6.75 %), and plagioclase feldspar ranged from 0 to 8 % (average 3.5 %). Other detrital and lithic grains occur in a relatively small amount (< 1%) (Table 2).

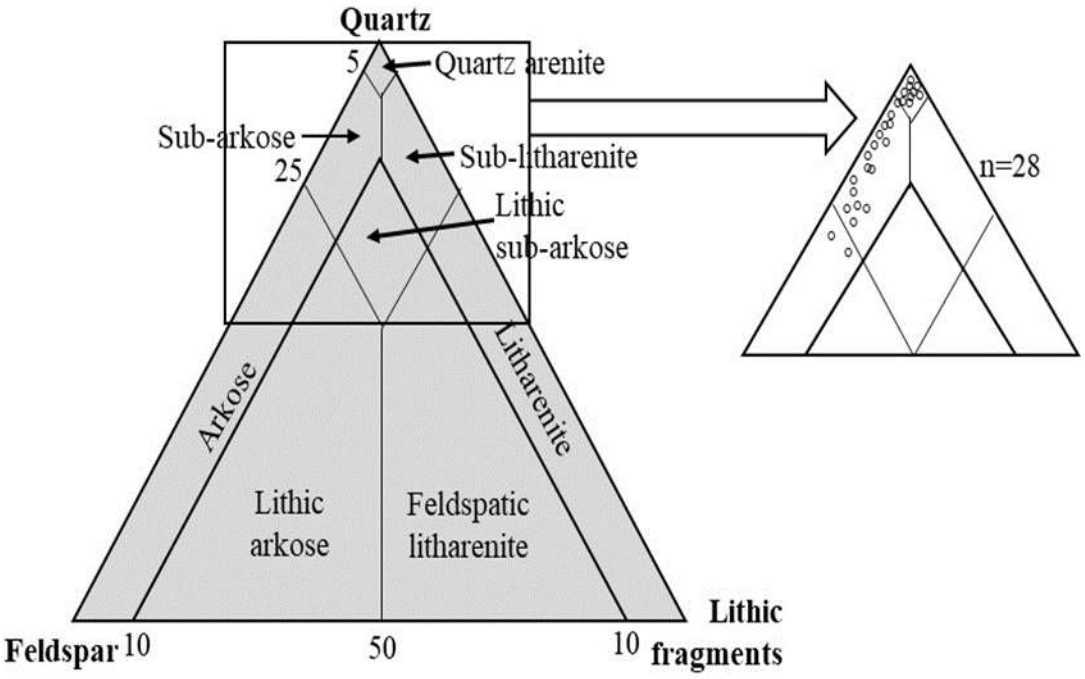

Figure 6- Ternary plot of classification after [26] of the Eze-Aku Group sandstones.

Clay Minerals

The authigenic clay minerals in the Eze-Aku sandstones, discernible from SEM images, include kaolinite, chlorite, illite, and smectite (Figure 7 a-d). The percentage composition of the clay minerals (identified from SEM) in each sample was deduced by visual estimation compared with the thin-section point count of minerals. They ranged from 6.0 % (at Abini bioturbated, deltaic sandstone) to 14.8 % (at Amasiri sandstone), an average of 9.5% (Table 3). The kaolinites in the Eze-Aku sandstones are quite visible on SEM images, often as well-defined booklets and/or vermicular clusters of clay matrix or cement. The chlorite minerals occurred as scattered plate-like crystals attached to quartz grain along their edges and were sometimes associated with kaolinite. On SEM image, Illite displays fibrous and hair-like crystal habit, while smectite exhibits web-like to boxwork crystal habit.

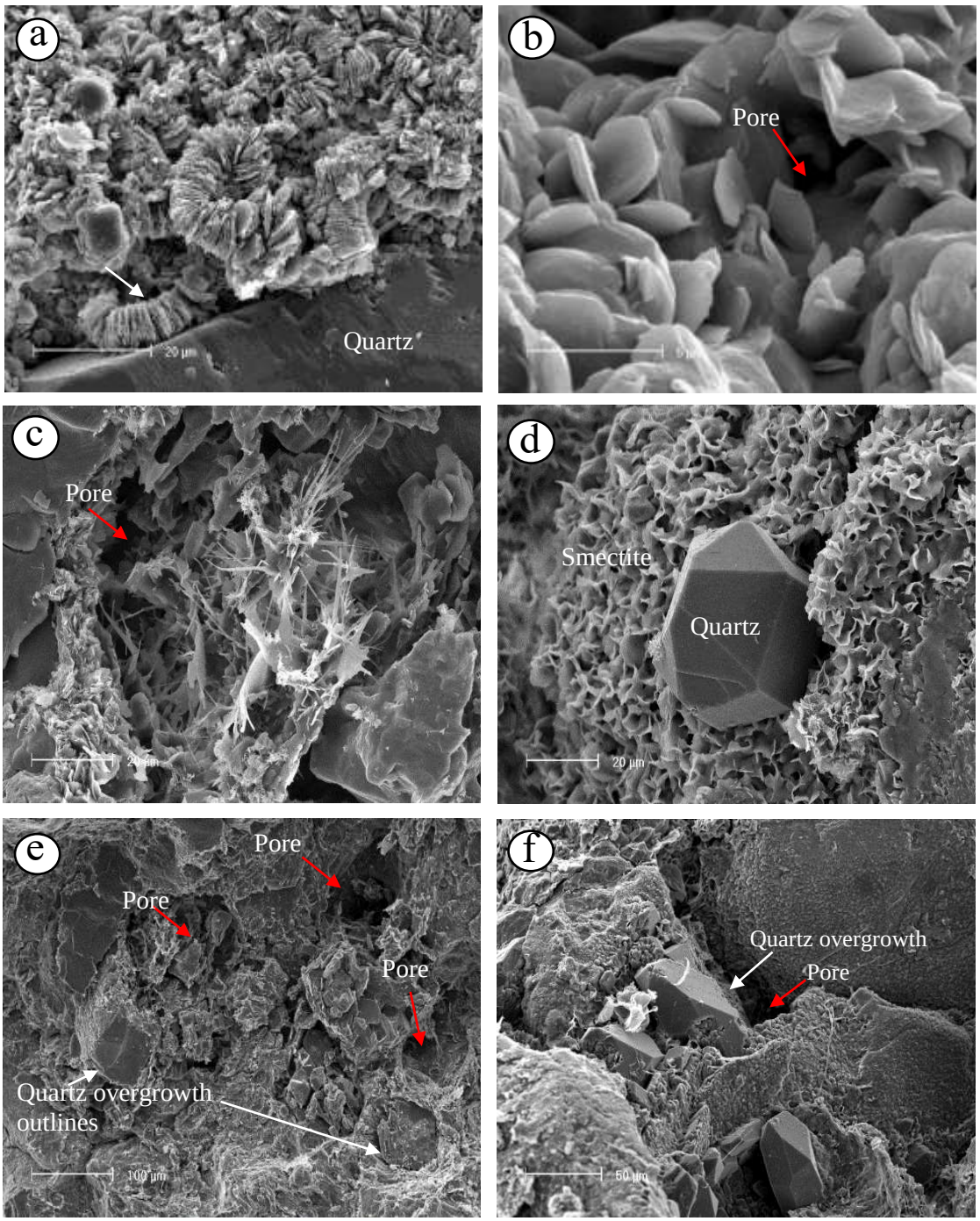

Figure 7- SEM images of mineral habits of the Eze-Aku sandstones. (a) Diagenetically induced crystalline pore-occlusion kaolinite booklets (white arrow) intergrown with quartz (with V-shaped indentations on the surface), (b) Chlorite (pore filling cement): occurring as scattered plate-like crystals attached to quartz grain along their edges, and intergrown with some authigenic kaolinites at the lower part of image, (c) Fibrous, pore (red arrow) bridging illite occurring in association with some smectite and quartz grains (upper left edge), (d) Smectite surrounding an euhedral quartz crystal, (e) Syntaxial overgrowth of quartz minerals (white arrowed), (f) Euhedral quartz overgrowth with some fibrous strands of illite on the bottom right hand side.

Discussion

Diagenesis and Pore Evolution

The diagenetic-related alterations and their effects on the reservoir characteristics of the Eze-Aku sandstones were inferred from the thin section petrography, SEM, and/or BSE image results. The relevant authigenic minerals closely related to these deductions include quartz overgrowths, clays, and felspar. They are quite invaluable in deducing the paragenesis (e.g., compaction, cementation, dissolution, replacement, etc.) of the Eze-Aku sandstone.

Compaction

It often occurs during the early transformational stage (eodiagenesis) of sediments to sedimentary rocks, marked by grain reorientation, repacking, dewatering, and porosity/permeability loss [21]. Determination of compaction from the thin section petrography involved evaluating the number of grain-to-grain (gtg) contacts and the shape of grain contacts. Taylor [27] reported <1.6 gtg contacts and 16.6 % 'floating grains' for uncompacted sands. He further stated that after up to 2.8 km burial, gtg contacts increase to >5, and shapes become increasingly complex. The Eze-Aku sandstones revealed gtg contacts of >5 and complex grain contacts (Figure 4 e-f), suggesting compaction and reduction in initial porosity.

Cementation

The sandstone shows that the quartz, clay, and feldspar cement occupy 50 %, 40 %, and 10 %, respectively. Quartz cement is abundant in the Eze-Aku sandstones as monocrystalline quartz overgrowths are rooted in detrital grains. On SEM images, they occurred as monocrystalline syntaxial quartz overgrowths (Figure 7e, f) with euhedral form or termination that grows into pore spaces.

Most authigenic clay cement is reported to have a distinctive pattern of pore filling, discrete, intergrown crystals, pore-lining, and pore bridging [27]. The kaolinite cement in the study samples is pore occluding, occurring on a spatial scale as a vermicular habit with clusters of booklets (Figure 7a). The chlorites identified in the Eze-Aku sandstones are monomineralic, scattered, plate-like, and pore-filling cement (Figure 7b). Ehrenberg [28] reported that chlorite coatings effectively inhibit quartz cement growth. In the study samples, illite cement (on SEM image) exhibits wispy and hair-like ends that are vertical to quartz grains or other detrital components. Also, they are fibrous, coating quartz grains and bridging intergranular pores (Figure 7c). The smectite cement in the samples studied are grain-coating, occluding, and surrounding euhedral quartz grains (Figure 7d). They appeared as intricate, crenulate, and honey-combed interlocked crystal habits.

Dissolution

Diagenetic processes are mostly responsible for secondary porosity and/or permeability development, either positively or negatively. The SEM BSE images suggested evidence of dissolution (Figure 8a & b). Chemical dissolution of quartz was inferred from V-shaped indentations in some study samples (Figure 7a). The partial and total dissolution of feldspars were observed in some of the SEM BSE images of the studied samples of the Eze-Aku sandstones. The partially dissolved feldspar grains exhibit rough outlines with micro-pores in the grain (intragranular), and in other cases, there is preferential leaching along cleavage planes and crystal twinning boundaries (Figure 8a & b). Total dissolution of feldspar was indicated by an apparent relict outline of the original mineral grain; almost all of the interior contents have been dissolved (Figure 8a). The dissolution of felspars and quartz likely introduced alumina and silica into the solution, precipitating as authigenic clays and quartz overgrowths.

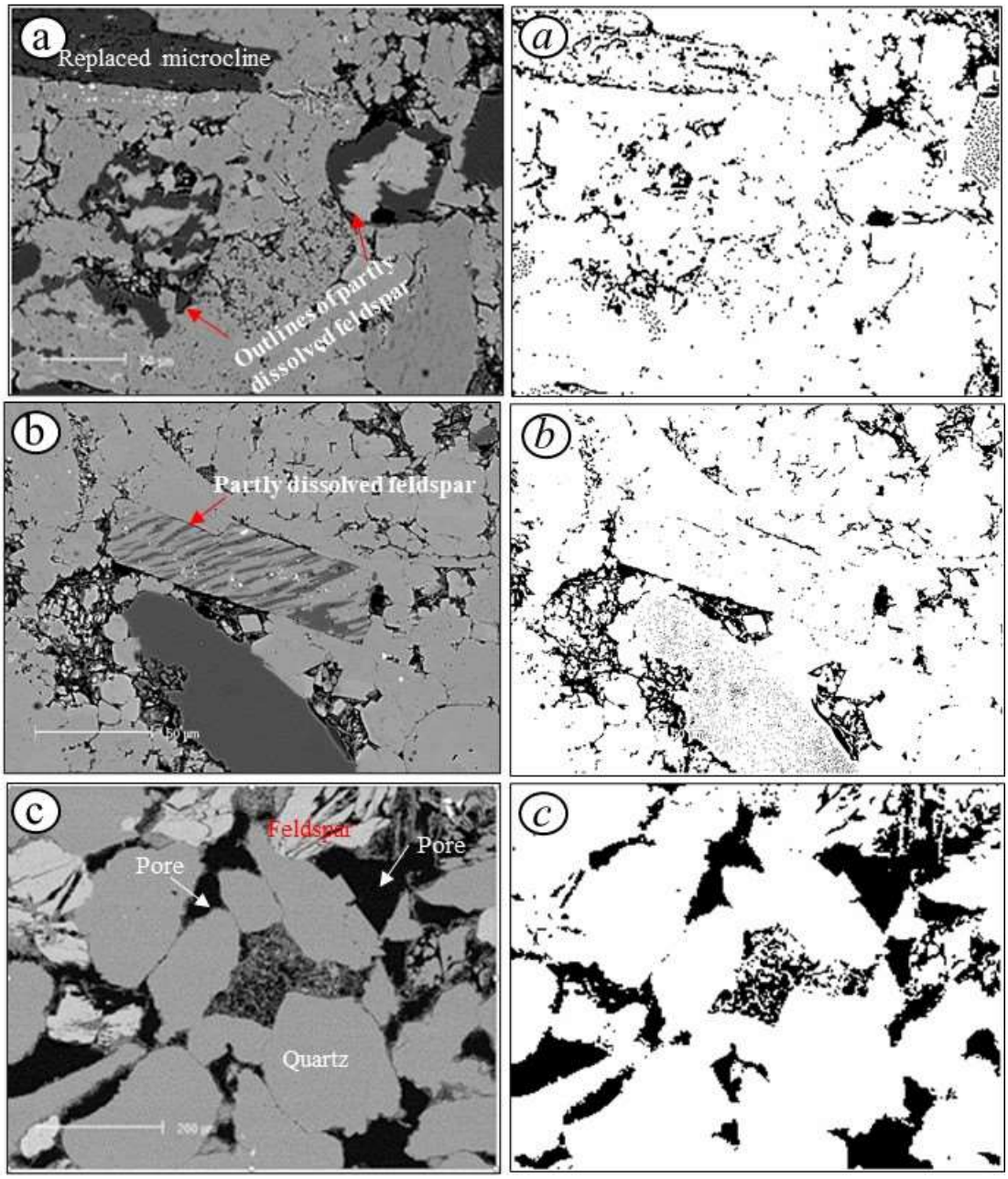

Figure 8- SEM Backscattered electron images (normal text labeled a to c) alongside their corresponding SEM BSE binarized images (for comparison and porosity determination) (italicized text labelled *a to c*) of the Eze-Aku sandstones; (a) Replacement of microcline and partial dissolution of feldspar, and (b) Partial dissolution of feldspar (note dissolved twinning boundaries, and (c) Loosely packed sandstone (pores white arrow),

Porosity and Permeability Estimation of the Eze-Aku Sandstone

Depositional porosity (intergranular) and secondary porosity types have been identified in the studied sandstones. Mechanical compaction and cementation have reduced the intergranular porosity (quartz cement and authigenic clays, e.g., kaolinite, illite, smectite, and chlorite). The intergranular porosity estimation was obtained through visually inspected and point-counted pore spaces on thin sections impregnated with blue epoxy resin (Figure 4f) and placed on a grid pattern microscope stage. The estimated intergranular porosity ranged

from15.6 to 24 % (av. 19.96 %) (Table 3). The SEM BSE images are also suitable for estimating porosity because they provide high contrast between quartz, feldspars, and pore spaces. A typical SEM BSE image often reveals quartz, feldspars, and pore spaces to be dark grey, light grey, and black (or very dark), respectively, based on their atomic-number contrast. The dark and light grey areas represent the minerals framework grains, matrix, and cement. On the SEM BSE images (Figure 8), the dark grey areas (representing quartz grains) are more than the light grey areas (representing feldspars), agreeing with the earlier petrographic result (through point counting) of average Q_{90} and F_{10}.

Table 3- Lithofacies, clay mineralogy, and estimated porosities of the Eze-Aku sandstones.

Formation	Lithology/no. of samples	Facies	Authigenic clays (av. %)	Porosity (av. %)
Agboha Igbo & Agbara Igbo	Sandstones, n = 4	Tidal channel, bioturbated sandstone.	10.0	16.8
Abini	Sandstone, n = 4	Deltaic, bioturbated sandstone.	6.00	23.7
Ugep	Sandstone, n =3	Deltaic, bioturbated sandstone	8.30	22.4
Ibii	Sandstone, n =3	R-T, bioturbated fine sandstone.	11.6	17.6
Abaomega	Sandstone, n = 3	R-T bioturbated, medium sandstone	12.4	15.6
Nko	Sandstone, n=3	Deltaic, bioturbated sandstone.	7.20	24.0
Amasiri	Sandstone, n =3	R-T calcareous bioturbated sandstone	14.8	19.0
Ozara Ukwu	Sandstone, n =3	Fluvial channel sandstone	6.90	20.6

R-T = Regressive-Transgressive barrier sand bodies (calcareous bioturbated); n = number of samples.

The image analysis was done using ImageJ to obtain porosity information from the SEM and BSE image data. Image analysis using the java-based software package ImajeJ involved a calibrated (to scale bar) 2-D grayscale SEM BSE image, subjected to binarization through proper thresholding, setting relevant measurement parameters (e.g., total area, fraction area, perimeter, percentage area, i.e., porosity, roundness, solidity, maximum and minimum area, diameter, i.e., ferret, etc.), and adjustment/measurement for porosity visualization [29] [30]. A binary digitally segmented image is produced that portrayed an individual spectrum of light grey (feldspars), dark grey (quartz), and black or very dark grey (pores). In figure 8, all the SEM BSE images (labelled a to c) were placed alongside their corresponding binarized images (labelled a to c in italics) for comparison.

The permeability values of the binarized SEM BSE images were calculated using the K-C equation. A modified form of K-C equation (i) proposed by [28] was used for the estimation. The equation is as follows:

$$K = \phi^3/C(1-\phi)^2(\frac{4PP}{\pi PA})^2 \ldots\ldots\ldots\ldots\ldots\ldots\ldots\ldots Equation\ (i)$$

Where; *K* is permeability in Md,
ϕ is porosity or area fraction in %,
c is constant = 7.65 (upper value of the pre-calcite pore system given by [28],
PP is pore perimeter (μm), and
PA is the pore area (μm^2).
The afore-listed parameters were obtained from image analysis using *Imagej*.

The results of the porosity and permeability measurements through image analysis are shown in Table 4. The sandstones revealed high porosity values of 19.7 to 25.5 % (average 22.7) and high permeability (range 34.44-1690 mD, average 745.43 mD). The range of porosity values did not vary so much compared to the permeability values that vary widely, attributable to variations in pore sizes/types. These values are generally classified as good to

very good (on average, very good) porosity. The permeability values are moderate to excellent (on average very good). The reservoir properties of the Eze-Aku sandstone are thus very good in their present outcropping state.

Table 4- Estimated petrophysical parameters from SEM BSE image analysis.

Sample #	Total area (μm^2)	Pore area (μm^2)	Area fraction (Porosity, %)	Pore perimeter (µm)	Permeability (k in mD)
Ez-1	120000	25800	21.60	948	1419.4
Ez-2	63100	14400	22.80	950	462.42
Ez-3	33200	8290	25.00	2090	34.440
Ez-4	329000	65000	19.70	2100	1690.3
Ez-5	119000	30000	25.20	2100	450.03
Ez-6	30600	6700	21.90	2090	415.97
Range/ (Average)	30600-329000 (115816.7)	6700-65000 (25031.67)	19.7-25.2 (22.7)	948-2100 (1713)	34.44-1690 (745.43)

The mineralogical composition of the Eze-Aku sandstone has been affected by diagenetic processes, affecting the petrophysical characteristics through total to partial dissolution of some feldspar grains. The resultant effect is secondary porosity and generation of aluminium and silica. However, the abundance of quartz grains constituted a stabilization framework against severe petrophysical deterioration of the sandstone. Although total to partial feldspar dissolution was recorded in some grains, the abundance of quartz grains stabilization framework supposedly withstood further mechanical compaction. Also, the dissolution products, silica and aluminium ions, precipitated as authigenic clays and silica cement [31] [32], further strengthening the Eze-Aku sandstone reservoir framework.

Conclusions

- The Eze-Aku sandstone was classified as sub-arkose with a $Q_{90}F_{10}L_0$ average modal composition based on thin-section petrography, confirmed by SEM BSE image analysis.
- Reservoir quality (in the case of porosity) does not vary significantly (19.7-25.2 %), while permeability varies significantly (34.44-1690 mD) due to the variations in overall pore sizes and types.
- The reservoir quality has been influenced by diagenetic processes such as compaction, cementation, and dissolution, although the abundance of quartz grain stabilization framework minimizes the level deterioration.
- Very good reservoir qualities are preserved in the Eze-Aku sandstone, an invaluable element for further hydrocarbon exploration in the Cretaceous inland basin that is yet to record any significant oil/gas discovery.

Compliance with ethical standards

1) Conflict of interest: Authors declare that they have no conflict of interest.

2) Ethical approval: This article does not contain any studies with human participants or animals performed by any authors.

Acknowledgements

This work was funded by the University of Port Harcourt and the O.B. Lulu-Briggs Chair. We the University of Liverpool for assisting with the laboratory analyses (thin section petrography and scanning electron microscopy). We also appreciate Professor Marshall and the laboratory staff of the University of Liverpool, who helped to source relevant research articles, even from other universities, to enhance this work.

References

[1] L. B. Magoon and W. G. Dow, "The Petroleum system," in The Petroleum system- from source to trap, vol. 60, L. B. Magoon and W. G. Dow, Eds., Okhlahoma, *American Association of Petroleum Geologists Memoir,* 1994, pp. 1-24.

[2] D. Morse, "Siliciclastic Reservoir Rocks," in The petroleum system- from source to trap, L. B. Magoon and W. G. Dow, Eds., Tulsa, Oklahoma: *American Association of Petroleum Geologists Memoir*, vol. 60, 1994, pp. 121-139.

[3] K. T. Biddle and C. C. Wielchowsky, "Hydrocarbon Traps," in The petroleum system- from source to trap, vol. 60, L. B. Magoon and W. G. Dow, Eds., Tulsa, Okhlahoma: American Association of Petroleum Geologists Memoir, 1994, pp. 219-235.

[4] R. H. Worden and S. D. Burley, "Sandstone diagenesis: the evolution of sand to stone," in Sandstone Diagenesis: Recent and Ancient, vol. (IAS Reprint Series 4), S. D. Burley and R. H. Worden, Eds., Oxford, Oxford Publishing Ltd, 2003, pp. 3-44.

[5] A. M. Salem, S. Morad, F. M. Mato and I. S. Al-Aasm, "Diagenesis and Reservoir-Quality Evolution of Fluvial Sandstones During Progressive Burial and Uplift: Evidence from the Upper Jurassic Boipeba Member, Recôncavo Basin, North-eastern Brazil," American Association of Petroleum Geologist Bulletin, vol. 84, no. 7, pp. 1015-1040, 2000.

[6] M. I. Odigi, "Diagenesis and reservoir quality of Cretaceous sandstones of Nkporo Formation (Campanian) south-eastern Nigeria," *Journal of Geology and Mining Research*, vol. 3, no. 10, pp. 265-280, 2011.

[7] M. I. Odigi, "Sedimentology of the Nkporo Campanian-Maastrichtian Conglomeratic Formation, Afikpo Sub-basin, South-eastern Benue Trough, Nigeria," *Nigerian Journal of Mining and Geosciences Society*, vol. 48, no. 1, pp. 45-55, 2012.

[8] Shell-British Petroleum (BP), "Map," 1967.

[9] R. A. Reyment, Aspects of the Geology of Nigeria, Ibadan: University of Ibadan Press, 1965, p. 145P.

[10] I. Banerjee, "A subtidal bar model for the Eze-Aku sandstones, Nigeria," *Sedimentary Geology* , vol. 25, no. 4, pp. 291-309, 1980.

[11] L. Amajor, "The Eze-Aku sandstone ridges (Turonian) of south-eastern Nigeria: A re-interpretation of their depositional origin," *Journal of Mining and Geology*, vol. 23, pp. 17-26, 1987.

[12] [R. Murat, "Stratigraphy and palaeogeography of the Cretaceous and Tertiary in Southern Nigeria," in African Geology, F. J. Dessauvagie and A. J. Whiteman, Eds., Ibadan, University Press, 1972, pp. 251-268.

[13] J. Benkhelil, "The origin and evolution of the Cretaceous Benue Trough (Nigeria)," *Journal of African earth sciences*, vol. 8, no. 2-4, pp. 251-282, 1989.

[14] U. A. Lar, T. P. Bata, H. U. Dibal, R. I. Daspan, L. C. Isah, A. A. Fube and D. A. Bassi, "Field, petrographic and geochemical study of basement, clastic and carbonate petroleum reservoirs in the northern Benue Trough, Nigeria," *Petroleum Technology Development Journal*, pp. 36-52, 2018.

[15] S. Nwachukwu, "The tectonic evolution of the southern portion of the Benue Trough, Nigeria," *Geological Magazine*, vol. 109, no. 5, pp. 411-419, 1972.

[16] M. Odigi, "Facies Architecture and Sequence Stratigraphy of Cretaceous formations, south-eastern Benue trough, Nigeria," Unpublished Ph.D. Thesis, University of Port Harcourt, Nigeria 2007.

[17] M. I. Odigi and L. C. Amajor, "Petrology and Geochemistry of sandstones in the southern Benue Trough of Nigeria: Implications for provenance and tectonic setting," *Chinese Journal of Geochemistry*, vol. 27, no. 1, pp. 384-394, 2008.

[18] M. I. Odigi and L. C. Amajor, "Geochemical characterization of Cretaceous Sandstone sequences from the southern Benue Trough, Nigeria.," *Chinese Journal of Geochemistry*, vol. 28, no. 1, pp. 49-54, 2009.

[19] S. O. Akande, A. Hoffknecht, and B. Erdtmann, "Environment of ore formation and anchizonal metamorphism in Pb-Zn-fluorite-barite deposits of the Benue Trough, Nigeria," *Geologie en Mijnbouw*, vol. 71, pp. 131-144, 1992.

[20] E. O. Igwe and A. U. Okoro, "Field and lithostratigraphic studies of the Eze-Aku Group in the Afikpo Synclinorium, southern Benue Trough, Nigeria," *Journal of African Earth Sciences*, vol. 119, pp. 38-51, 2016.

[21] D. S. Umer-Scholle, P. A. Scholle, J. Schieber and R. J. Raine, Colour Guide to the Petrography of Sandstones, Siltstones, Shales, and Associated Rocks, Tulsa, Oklahoma: American Association of Petroleum Geologists Memoir, vol. 109, 2015, p. 543P.

[22] K. Ruzyla, "Characterisation of pore space by quantitative image analysis," *Formation Evaluation*, vol. 1, pp. 389-398, 1986.

[23] N. Trewn, "The SEM in Sedimentology," in Techniques in sedimentology, M. E. Tucker, Ed., Oxford, Blackwell Science Publications, 1988, pp. 86-107.

[24] J. Evans, A. C. Hogg, M. S. Hopkins and R. J. Howarth, "Quantification of quartz cement using combined SEM, CL, and image analysis," *Journal of Sedimentary Research*, vol. 64, no. 2a, pp. 334-338, 1994.

[25] C. A. Schneider, W. S. Rasband and K. W. Eliceiri, "NIH Image to ImageJ: 25 years of image analysis," *Nature Methods*, vol. 9, no. 7, pp. 671-675, 2012.

[26] E. F. McBride, "A classification of common sandstones," *Journal of Sedimentary Research*, vol. 33, pp. 664-669, 1963.

[27] J. M. Taylor, "Pore-space reduction in sandstones vol. 34, no. 4," American Association of Petroleum Geologists Bulletin, vol. 34, no. 4, pp. 701-716, 1950.

[28] S. Ehrenberg, "Preservation of anomalously high porosity in deeply buried sandstones by grain-coating chlorite: Examples from the Norwegian continental shelf," American Association of Petroleum Geologists Bulletin, vol. 77, no. 7, pp. 1260-1286, 1993.

[29] M. Mowers and D. A. Budd, "Quantification of Porosity and Permeability Reduction Due to Calcite Cementation Using Computer-Assisted Petrographic Image Analysis Techniques," American Association of Petroleum Geologists Bulletin, vol. 80, no. 3, pp. 309-321, 1996.

[30] J. M. Rine, E. Smart, W. Dorsey, K. Hooghan and M. Dixon, "Comparison of porosity distribution within selected North American shale units by SEM examination of Argon-ion-milled samples," in Electron microscopy of shale hydrocarbon reservoirs, W. Camp, E. Dianz and B. Wanak, Eds., Tulsa, Oklahoma: American Association of Petroleum Geologists Memoir, vol. 102, 2013, pp. 137-152.

[31] E. Mc Bride, "Quartz cement in sandstones: a review," *Earth-Science Reviews*, vol. 26, no. 1-3, pp. 69-112, 1989.

[32] M. W. French, R. H. Worden, H. E. King, W. C. Horn, W. A. Lamberti and J. D. Shosa, "The origin of silica cements revealed spatially resolved oxygen isotope microanalysis and electron-beam microscopy; Heidelberg Formation, Germany," Geochimica et Cosmochimica Acta, vol. 309, pp. 57-78, 2021.